Dielectric optical interfaces in total internal reflection for ultrasound detection

E. O. Carrillo Vallejo, C. G. Carreño Romano
GLOmAe, Depto. Física, FI
Universidad de Buenos Aires
CABA, Argentina
ecarrillo.ext@fi.uba.ar, ccarreno@fi.uba.ar

F. E. Veiras and L. Ciocci Brazzano
GLOmAe, Depto. Física, FI
Universidad de Buenos Aires, CONICET
CABA, Argentina
fveiras@fi.uba.ar, bciocci@fi.uba.ar

***Abstract*—In this work we carry out a detailed analysis of the design and performance of an optical quasi-point ultrasound detector for optoacoustic tomography. The detector is a two-dielectric system based on a glass prism (for light coupling) and water. The behaviour of the system is analyzed for six different modes of operation that arise from monitoring the amplitude and phase of the electric field of the reflected optical beam. For both amplitude and phase monitoring, we consider modes of operation centered on parallel and perpendicular components of the electric field individually and a differential mode (parallel-perpendicular). For each operation mode, we estimate the best set of parameters (refractive indices and angle of incidence). We verify that the optimum performance, in terms of sensitivity, is obtained when the angle of incidence of the interrogation beam is close to the critical angle. The best performance for operation modes based on monitoring an individual parameter is obtained by means of glass prisms with low refractive index, whereas for differential modes of operation higher refractive indices are preferred. We verify the linearity of each configuration by means of the numerical calculation of the total harmonic distortion**

***Index Terms*—ultrasound transducers, optical sensors, optical interfaces, total internal reflection**

I. Introduction

Optical ultrasound detectors have several advantages in biomedical applications, such as remote and non-contact inspection, and immunity to electromagnetic interference [1], [2]. The use of fiber optics and free-space optical sensors with different detection geometries is widely spread in optoacoustic tomography (OAT) [3], [4], [5]. In particular, the geometry of quasi-point sensors does not restrict the bandwidth of operation, therefore making the study and design of photodetection systems for sensors based on optical properties of interfaces very attractive for OAT. For example, these systems can be implemented by means of a three-layer structure as in the case of plasmonic sensors [6] or they can be based on an interface between two dielectrics [7]. These systems allow us to sense ultrasonic pressure waves in water using an interrogation beam that incides on an interface at a fixed angle and wavelength. Therefore, the detection system is focused on monitoring the properties of the reflected beam.

Identify applicable funding agency here. If none, delete this.

II. Theoretical Background

In Fig. 1 we show the scheme of a quasi-point ultrasound sensor. An incident beam with light intensity I_0 incides on an interface formed by a glass prism (with refraction index n_1) and water (with refraction index n_2). The characteristics of the reflected beam depend on the Fresnel coefficients associated to the interface [8]. For a glass-water interface, since the condition $n_1 > n_2$ holds, there is always a critical angle θ_{crit}. For angles of incidence lower than θ_{crit}, the coefficients, for both s and p components, are real and depend on n_1, n_2, and the angle of incidence (α). Therefore, the reflectivities are

$$r_s = \left| \frac{n_1 \cos\alpha - n_2 \cos\left[\arcsin\left(\frac{n_1 \sin\alpha}{n_2}\right)^2\right]}{n_1 \cos\alpha + n_2 \cos\left[\arcsin\left(\frac{n_1 \sin\alpha}{n_2}\right)^2\right]} \right|^2 \tag{1a}$$

$$r_p = \left| \frac{n_2 \cos\alpha - n_2 \cos\left[\arcsin\left(\frac{n_1 \sin\alpha}{n_2}\right)^2\right]}{n_1 \cos\alpha + n_2 \cos\left[\arcsin\left(\frac{n_2 \sin\alpha}{n_1}\right)^2\right]} \right|^2 \tag{1b}$$

As shown in the upper panel of Fig. 2, as angle of incidence approaches to θ_{crit}, the reflectivity, rapidly rise to 1.

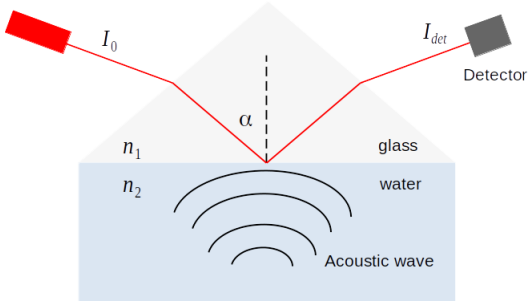

Fig. 1. Ultrasound detection scheme.

For angles of incidence higher than θ_{crit}, the coefficients became complex valued, with modulus one, and the phenomenon is then referred to as total internal reflection (TIR). In this case, the argument of the coefficients depends on the same parameters:

$$\delta_s = -2\arctan\frac{\sqrt{\sin^2\alpha - \left(\frac{n_2}{n_1}\right)^2}}{\cos\alpha} \tag{2a}$$

$$\delta_p = -2\arctan\frac{\sqrt{\sin^2\alpha - \left(\frac{n_2}{n_1}\right)^2}}{\left(\frac{n_2}{n_1}\right)^2\cos\alpha} \tag{2b}$$

As shown in the lower panel of Fig. 2, as the angle of incidence approaches θ_{crit}, they rapidly rise from 0. In Fig.2 we plot the module and phase of the coefficients for 5 different commercial glasses (n_1=1.48, 1.56, 1.66, 1.72, and 1.84) and pure water (n_2=1.33) at $\lambda = 632.8$ nm. The magnitude and phase of the coefficients, (1) and (2), depend on the value of the refractive index of the water in the vicinity of the intersection of the incident beam with the interface. Therefore, it can be regarded as a quasi-point sensor whose geometry can be controlled by means of the characteristics of the incident beam. Moreover, for small pressure signals (as in OAT) it could be employed as quasi-point ultrasound sensor due to the dependence of the refractive index on the pressure:

$$n_2 = n_{20} + \frac{\mathrm{d}n_2}{\mathrm{d}p}\Delta p_0 \tag{3}$$

where n_{20} is the refractive index in absence of disturbances, $\frac{\mathrm{d}n_2}{\mathrm{d}p} = 1.32\times10^{-10}\mathrm{Pa}^{-1}$,and Δp_0 is the difference between the instantaneous pressure and the equilibrium pressure.

III. Detection Modes

Eq. (3) shows that ultrasonic pressure pulses can be matched to refractive index changes Δn_2. Therefore, as a change in the refractive index produces a change in the intensity of the reflected beam, a first order Taylor approximation shows that a detection system monitoring the reflected beam, working at a fixed wavelength and angle of incidence, can sense small amplitude pressure waves

$$\Delta I_{det} \cong \frac{\mathrm{d}I_{det}}{\mathrm{d}n_2}\Delta n_2 \tag{4}$$

As shown in Sec. II, for angles of incidence lower than θ_{crit} the system tracks changes in the amplitude of the reflected beam, whereas for angles of incidence greater than θ_{crit} (TIR) the system tracks changes in the phase of the reflected beam. In the first case, a photodetection system directly senses the intensity variations of the reflected beam

$$\Delta I_{det} \cong \frac{\mathrm{d}I_{det}}{\mathrm{d}r}\frac{\mathrm{d}r}{\mathrm{d}n_2}\Delta n_2 = I_0\frac{\mathrm{d}r}{\mathrm{d}n_2}\Delta n_2, \tag{5}$$

where I_0 is the intensity of the incident beam, and $\frac{\mathrm{d}r}{\mathrm{d}n_2} = S_r$, the sensitivity. Therefore, the system can be configured to sense the intensity associated with the p and s components of the reflected beam. Moreover, in order to mitigate the effects of intensity fluctuations a differential mode can also be implemented. The upper panel of Fig. 3 shows the reflectivity r_s as a function of the refraction index n_2 around the value

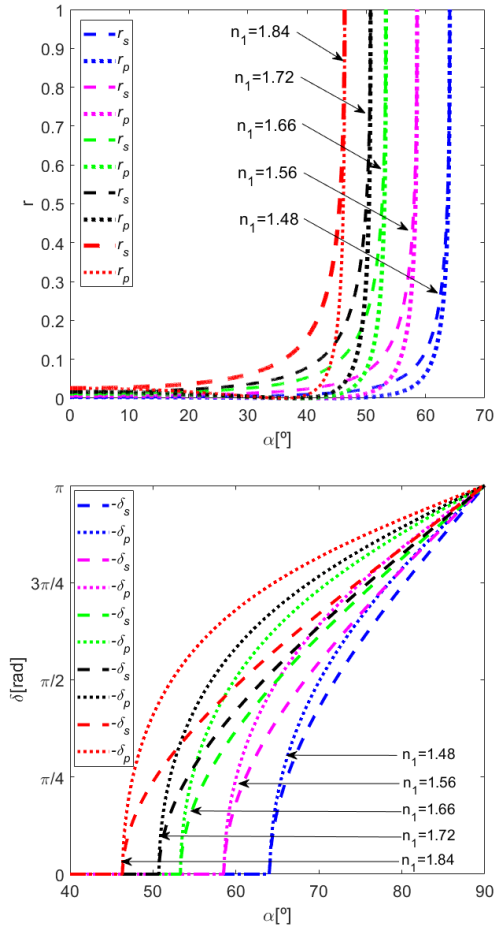

Fig. 2. Module (upper panel) and phase (lower panel) of the coefficients (p and s components of the reflected beam) for 5 different commercial glasses and n_2=1.3311.

that corresponds to water in equilibrium (i.e. n_2=1.3311). The correlation coefficient is close to unity and validates the first order approximation. A similar linear behaviour is also observed for r_p. It is worth noting that both r_p and r_s monotonously decrease and therefore r_{s-p} also shows a linear behaviour but with a smaller slope.

In the second region, the argument of the coefficient is also sensitive to fluctuations of the refractive index Δn_2. In TIR the amplitude of the reflected beam does not change and therefore an optical interferometer has to be arranged in order to translate the phase changes into intensity variations of an optical beam

$$\Delta I_{det} \cong \frac{\mathrm{d}I_{det}}{\mathrm{d}\delta}\frac{\mathrm{d}\delta}{\mathrm{d}n_2}\Delta n_2. \tag{6}$$

For comparison purposes we propose an ideal two beam null interferometer with equal intensities in each arm ($I_0/2$ correspondingly). This kind of interferometer is adjusted to its maximum response (i.e., maximum intensity variations for phase differences) when a $\pi/2$ offset phase signal between both arms is set. Therefore, (6) becomes

$$\Delta I_{det} \cong I_0 \frac{\mathrm{d}\delta}{\mathrm{d}n_2} \Delta n_2, \tag{7}$$

where $\frac{\mathrm{d}\delta}{\mathrm{d}n_2} = S_\delta$, is the sensitivity. Therefore, the system can be configured to sense the ultrasonic pressure pulses associated with the phase of the p and s components of the reflected beam. It is worth noting that the differential mode can be easily implemented by just placing a quarter wave plate and a polarizer across the reflected beam to produce the desired interference. The lower panel of Fig. 3 shows the phase δ_s as a function of the refraction index n_2 around the value that corresponds to water in equilibrium (i.e. n_2=1.3311). The correlation coefficient is also close to unity and validates the first order approximation. A similar linear behaviour is again observed for the p component. Similar considerations also apply to the differential phase mode δ_{s-p} (i.e. linear behaviour with lower slope).

Both (5) and (7) show a similar behaviour and set the designers attention to the optimization in terms of the sensitivity S (either amplitude or phase sensitivity).

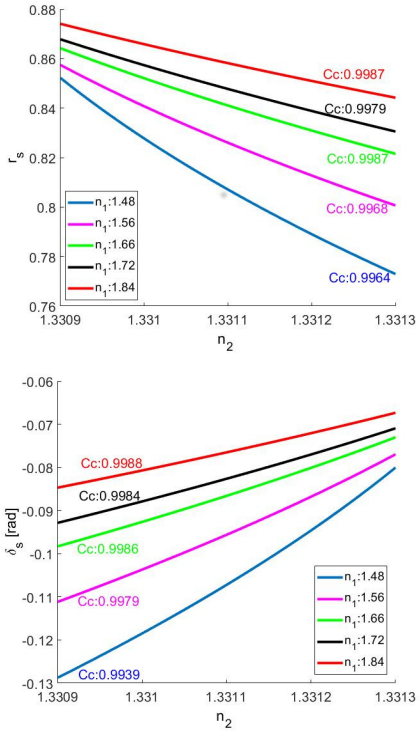

Fig. 3. Reflectivity (upper panel) and phase (lower panel), as a function of the refraction index around the value that corresponds to water in equilibrium (i.e. n_2=1.3311). $|\alpha - \theta_{crit}| = 0.04°$.

IV. Numerical Results

Sensitivity can be adjusted by means of the index of refraction n_1 and the angle of incidence α. Fig. 4 shows the sensitivity as a function of the angle of incidence for the s component of the reflected beam in both amplitude (upper panel) and phase (lower panel) detection modes. As expected, the behaviour shows that as the incidence is closer to θ_{crit}, the sensitivity increases. We consider an impinging beam with a typical Gaussian profile from a He-Ne 632.8 nm laser with an angular divergence of $0.04°$. Therefore, in order to ensure that the system is operating in either one region or the other, we evaluate angles of incidence such that $|\alpha - \theta_{crit}|$ is lower than $0.04°$. Similar trends are observed for detection modes based on the p component but with higher values of sensitivity.

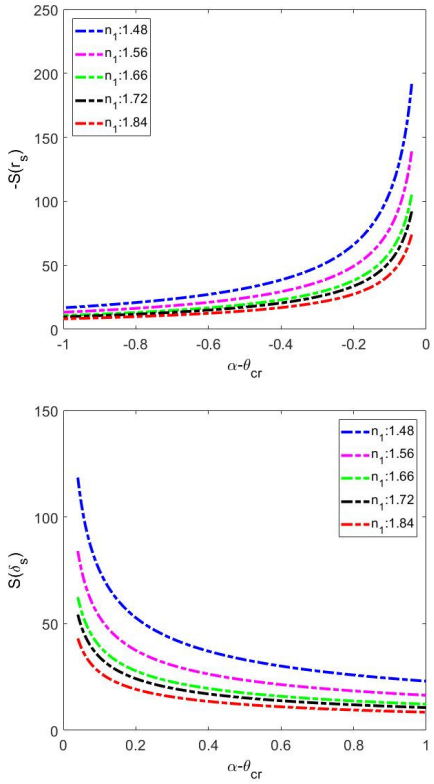

Fig. 4. Sensitivity as a function of the angle of incidence for the s-component. Amplitude sensitivity $-S_{rs}$ (upper panel) and phase sensibility $S_{\delta s}$ (lower panel). n_2=1.3311.

For detection modes based on a single component (s or p), the higher values of sensitivity are obtained with the lower refractive index prisms. However, as the refractive index n_1 decreases, θ_{crit} increases and for higher sensitivity, grazing incidence may be required. In the case of the differential modes (either amplitude or phase), the behaviour of the sensitivity curves is similar but they reach lower sensitivities. Additionally, the higher sensitivities are reached with higher refraction index prisms.

Since the sensitivity increases as the angle of incidence gets closer to the critical angle it is interesting to have a quantitative measure of the behaviour regarding linearity such as THD as a function of the signal amplitude. We tested each configuration with a 100 cycles sinusoidal excitation with 100 samples per cycle (i.e., 10 kSamples) and calculated the THD for each amplitude. As shown in Fig. 5 the calculated points of the porcentual THD (THD%) perfectly fit a parabola with the vertex at the origin (THD% = a (Amplitude)^2). Therefore

the THD% can be directly calculated from its quadratic coefficient, a. Table I shows a summary of the numerical results of the configurations with higher sensitivity for each detection mode at 632.8 nm. Each of them is evaluated at an angle of incidence of 0.04 ° and 1 ° from the critical angle. For single component detection modes (r_s,r_p,δ_s, or δ_p) the refractive index used for calculations corresponds to FK51A (n_1=1.48), whereas for differential modes the prism material is LASF9 (n_1=1.84).

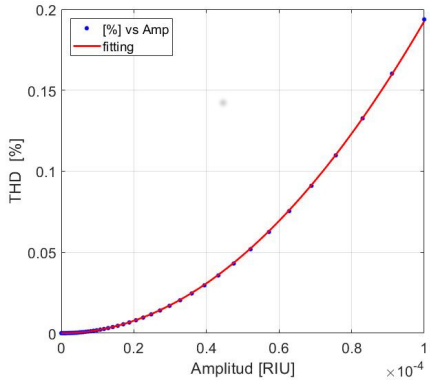

Fig. 5. THD% as a function of the amplitude of the disturbance in RIU.

On the one hand, the single component detection modes based on the p component present higher sensitivities (225 for amplitude and 145 for phase) than the ones based on the s component (192 for amplitude and 118 for phase). On the other hand, the amplitude detection modes present higher sensitivities than those based on phase. In comparison, differential modes can help mitigate noise but present lower sensitivities (below 50). The THD increases with the angle of incidence but, as shown in Table I, the maximum amplitudes without surpassing a maximum THD% of 0.1% is kept below the fourth digit of the refraction index of water (i.e. pressure amplitudes up to 500 kPa). This indicates that all of the configurations can measure pressure pulses for OAT without introducing a considerable amount of distortion.

TABLE I
SUMMARY

Angle (α)	**Prism**	**Det. mode**	**Sens.** S	**Constant** (a)	**Max. Amplitude (0.1%THD) [RIU]**
64.03	FK51A	r_s	192	1.17×10^7	9.3×10^{-5}
		r_p	225	1.27×10^7	8.9×10^{-5}
63.07	FK51A	r_s	17	4.56×10^4	1.5×10^{-3}
		r_p	16	6.05×10^4	1.3×10^{-3}
64.11	FK51A	δ_s	118	7.67×10^6	1.1×10^{-4}
		δ_p	145	7.65×10^6	1.1×10^{-4}
65.07	FK51A	δ_s	23	1.69×10^4	2.4×10^{-3}
		δ_p	28	1.62×10^4	2.5×10^{-3}
46.30	LASF9	r_{s-p}	49	1.93×10^7	7.2×10^{-5}
45.34	LASF9	r_{s-p}	0.5	1.48×10^5	8.2×10^{-4}
46.38	LASF9	δ_{s-p}	36	1.48×10^6	2.6×10^{-4}
47.34	LASF9	δ_{s-p}	7	3.71×10^5	5.2×10^{-4}

V. CONCLUSIONS

In this paper we described and analyzed an optical quasi-point ultrasound detector for OAT. It is based on monitoring the properties of an optical beam reflected on an interface between a glass prism and water. The system operates at a fixed angle and wavelength. We found six detection modes based on amplitude and phase. OAT is a technique of ultrasound imaging that requires the measurement of low amplitude and large bandwidth pressure pulses from several positions in space without introducing significant levels of distortion. Therefore, the geometry of the sensing region, the sensitivity and the linearity of the sensor are of critical importance. We evaluated the performance in terms of sensitivity and THD for a wide range of commercial glass prisms. The results evidence that as the angle of incidence is closer to the critical angle the sensitivity is higher. In comparison, the sensitivities obtained with detection modes based on the amplitude of the reflected beam are higher than those based on their phase. The differential modes of operation (either amplitude or phase) present some benefits regarding noise reduction but they present a lower sensitivity in comparison with the modes based on a single parameter. In the former the higher sensitivities are obtained with prisms with the higher index of refraction. In the latter, the higher sensitivities are obtained with the prisms with the lower index of refraction. Moreover, for the configurations with the highest sensitivity, operating at an angle of incidence at 0.04 °s from the critical angle, the THD is kept below 0.1% for pressure amplitudes up to 500 kPa.

ACKNOWLEDGMENT

This work was supported by UBA (UBACyT grants 20020160100052BA, 20020170200232BA, 200201901000275BA, and 20020190200255BA) and by ANPCyT (PICT grants 2016-2204 and 2018-04589).

REFERENCES

[1] B. Dong, C. Sung and H.F. Zhang, "Optical Detection of Ultrasound in Photoacoustic Imaging", IEEE Trans. Biomed. Eng., vol. 64(1), pp 4–15, 2016.
[2] G. Wissmeyer, M. A. Pleitez, A. Rosenthal, and V. Ntziachristos, "Looking at sound: optoacoustics with all-optical ultrasound detection", Light Sci. Appl, vol. 7(1), pp 1–16, 2018.
[3] G. Paltauf, R. Nuster, M. Haltmeier, and P. Burgholze, "Photoacoustic tomography using a Mach–Zehnder interferometer as an acoustic line detector", Appl. Opt., vol. 46(16), pp 3352–3358, 2007.
[4] L.M. Riobó, F.E. Veiras, M.T. Garea, and P.A. Sorichetti "Software-Defined Optoelectronics: Space and Frequency Diversity in Heterodyne Interferometry" IEEE Sens. J., vol. 18(14), pp 5753–5760, 2018.
[5] L. Riobó, Y. Hazan, F. Veiras, M. Garea, P. Sorichetti, and A. Rosenthal, "Noise reduction in resonator-based ultrasound sensors by using a CW laser and phase detection", Opt. Lett., vol. 44(11), pp 2677–2680, 2019.
[6] R. D. Araguillin, L. Ciocci Brazzano, L. I. Perez, and F. E. Veiras, "Design of reflectivity-based surface plasmon resonance optical sensors for ultrasound detection" J. Mod. Opt., vol. 68(13) pp, 689–698, 2021.
[7] X. Zhu, Z. Huang, G. Wang, W. Li, D. Zou, and C. Li,"Ultrasonic detection based on polarization-dependent optical reflection", Opt. Lett., vol. 42(3), pp 439–441, 2017.
[8] M. Born and E. Wolf, "Principles of optics: electromagnetic theory of propagation, interference and diffraction of light" Elsevier, 2013.